объединенный
институт
ядерных
исследований
дубна

E2-82-426

V.V.Uzhinskii

SOME RESULTS OF THE NUCLEUS-NUCLEUS SCATTERING EIKONAL THEORY

Submitted to the XXI International Conference on High Energy Physics (Paris, 1982)

1982

How it's well known, Glauber's approximation was successfully used for the description of the elastic and inelastic hadron-nucleus scattering at high energies. In the last years many efforts have been made to extend and apply it for an analysis of the nucleus-nucleus interactions. The key problem here was to solve combinatorical questions, or classify scattering processes and to obtain a compact mathematical expression for the elastic scattering amplitude - $F_{AB}(\vec{q})$. To demonstrate the complication of this problem, let us represent a nucleus-nucleus collision in fig.1, where the circles correspond to the interacting nuclei, the black and light points to nucleons, the solid lines to interactions between nucleons. Now it can be seen that for a recountering all possible processes we have to pluck all possible combinations of the light and black points and the solid lines connecting them. To crown it all, we have to say how many of the combinations are in equivalence and how many classes of the equivalences exist.

It's quite clear that if the mass numbers A and B of two colliding nuclei are small, the number of combinations is not large. So we can take into account all of them.

In this way many calculations have been made. Some of them are shown in figs.2,3 (see also ref.[4]).

In the case when A and B are large, the problem becomes more complicated. But here it's easy to find the so-called phase function - $\chi(\vec{b})$

$$F_{AB}(\vec{q}) = \frac{iP_B}{2\pi} \int d^2b\, e^{i\vec{q}\vec{b}} [1 - e^{-\chi(\vec{b})}]. \qquad (1)$$

This was performed in papers[5,6] (see also refs.[7,8]). The main result is

$$\chi(\vec{b}) = \chi(\frac{\tilde{\sigma}}{2}, T_A, T_B) = \frac{2}{\tilde{\sigma}} \int d^2s \sum_{m,n=1} \frac{(-1)^{m+n}}{m!n!} \cdot m^{n-1} \cdot n^{m-1} \cdot x^m \cdot y^n =$$
$$= \frac{2}{\tilde{\sigma}} \int d^2s [u(e^z - 1) + z(e^u - 1) - uz], \qquad (2)$$

where $\tilde{\sigma} = \sigma_{tot}(1 - i\epsilon)$, σ_{tot} is the nucleon-nucleon scattering total cross-section; ϵ, the ratio of the real to imaginary

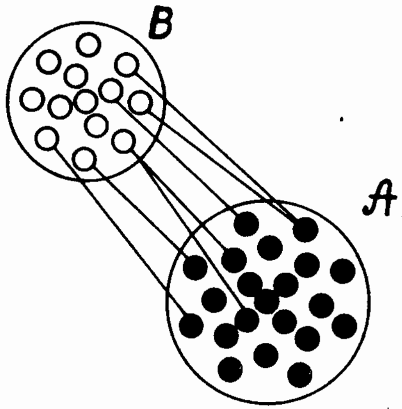

Fig.1. A picture of the nucleus-nucleus interaction in the impact parameter plane.

Fig.2. The differential cross-section of the $p\,{}^4He$- and ${}^4He\,{}^4He$-elastic scattering (figs. a,b and c,d, respectively) at the ISR. Points are the data from paper [1]. Lines are the calculations performed in the ordinary eikonal scheme [2].

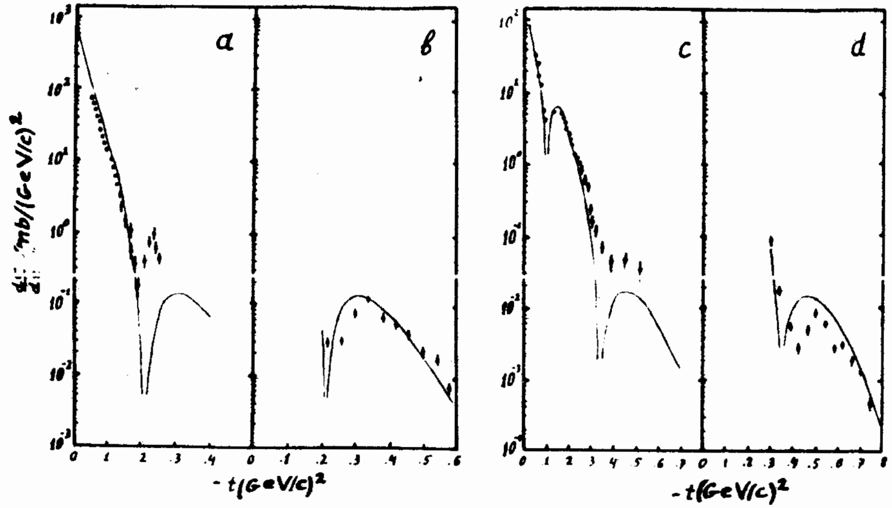

parts of the elastic nucleon-nucleon scattering amplitude at zero transversal momentum,

$$x = \frac{\tilde{\sigma}}{2} T_A(\vec{s}) \qquad y = \frac{\tilde{\sigma}}{2} T_B(\vec{b}-\vec{s}),$$

T_A and T_B are the thickness functions of the nuclei A and B, u and z are solutions of the system of equations

$$u = y e^{-z} \qquad (3)$$

$$z = x e^{-u}\,.$$

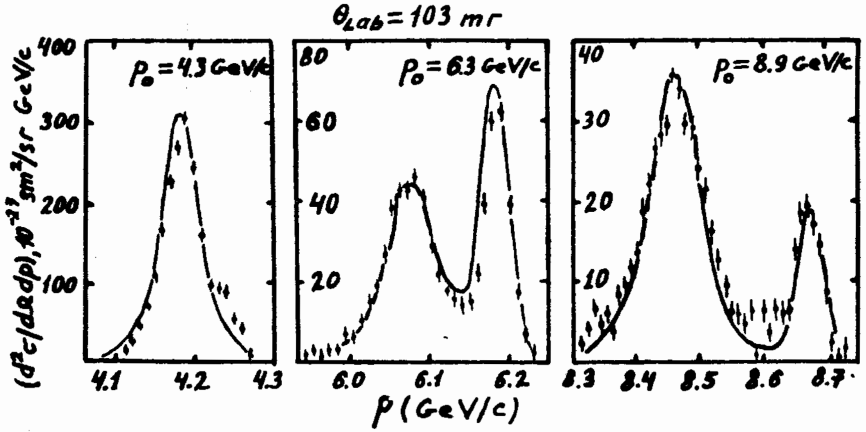

Fig.3. The momentum spectra of deuterons in the reactions $dd \to dx$. The experimental points and calculations are taken from ref. [3].

By using expression (2) the description of the data [9] was given (in figs.4,5). Now in this scheme one can calculate the cross-sections of the quasi-elastic nucleus-nucleus scattering, the charge-exchange reactions, excitation processes (fig.6) and estimate the influence of the short range correlations of the nucleons in nuclei [11], Coulomb effects [12], correlations caused by finite mass numbers, and so on.

The first and second calculation schemes were connected with the use of the graph theory in paper [2], where a general solution of the combinatorical problem was given. An application of the graph theory opens a new opportunity, in particular, the estimation of the inelastic shadowing effects: in the two-component nucleon model, the inelastic screening in the nucleus-nucleus scattering is taken into account by

$$\chi\left(\frac{\tilde{\sigma}}{2}, T_A, T_B\right) \to |c|^2 \chi\left(\frac{\tilde{\sigma}}{2|c|^2}, T_A, T_B\right),$$

where $|c|^2$ is a weight of the active state of the nucleon.

In figs.7,8 the predictions [2] of the inelastic shadowing effects in ${}^4He\,{}^4He$- and ${}^{40}Ca\,{}^{40}Ca$ -reactions are presented. As it can be seen, the effects grow with growing transversal momentum and we can expect that the differential cross-section of elastic scattering of heavy ions having energy about 400 GeV per nucleon in the lab.syst. in experiment will be much less than given by the ordinary eikonal theory. Note that the cross-sections of these reactions decrease very rapidly (fig.9).

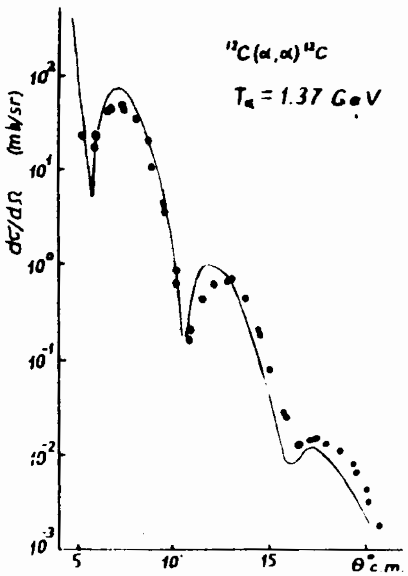

Fig.4. The differential cross-section of $^{4}He^{12}C$-elastic scattering. The points are the data from paper /9/. The calculation represented by the solid line is taken from /6/.

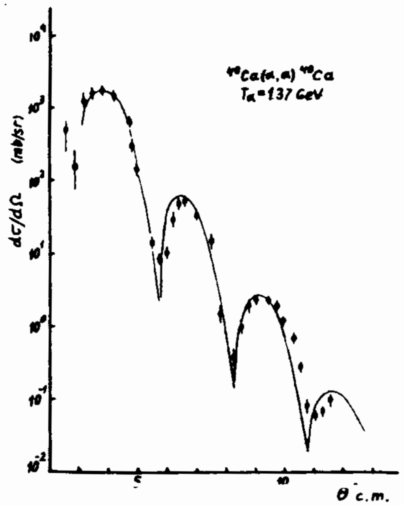

Fig.5. The same as in fig.4, but for $^{4}He^{40}Ca$-reaction. The points are the data from paper /10/.

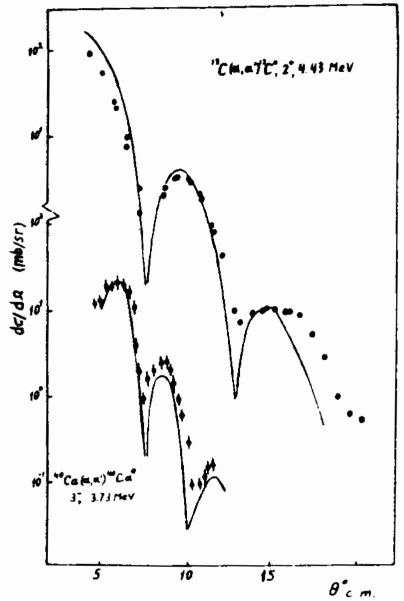

Fig.6. The excitation differential cross-sections of $^{4}He\,^{12}C$- and $^{4}He^{40}Ca$ -reactions. The points are the experimental data /9,10/; the solid lines, the calculations of. /6/.

So, their measurement requires high-resolution techniques, which will not work efficiently because many times they will wait for events and will dump inelastic collisions. The latter will be many in number. Thus it seems quite reasonable to investigate the elastic and inelastic interactions in common. But shall we be able to extract information from these data?

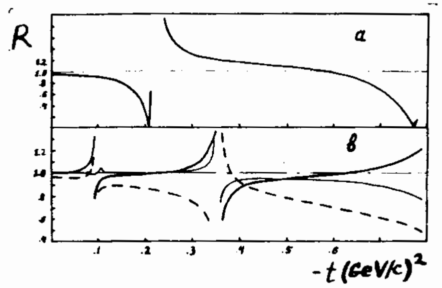

Fig.7. a) The ratio of two differential cross sections of the $p\,^{4}He$ -elastic scattering calculated with and without taking into account inelastic shadowing corrections. b) The dashed line represents the same ratio as in fig.a, but for $^{4}He\,^{4}He$ -elastic scattering in the ISR. The other lines demonstrate different theoretical approaches.

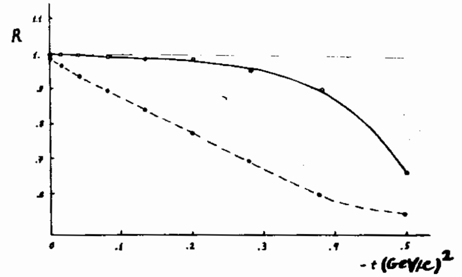

Fig.8. The same as in fig.7b, but for $^{40}Ca^{40}Ca$ -elastic scattering.

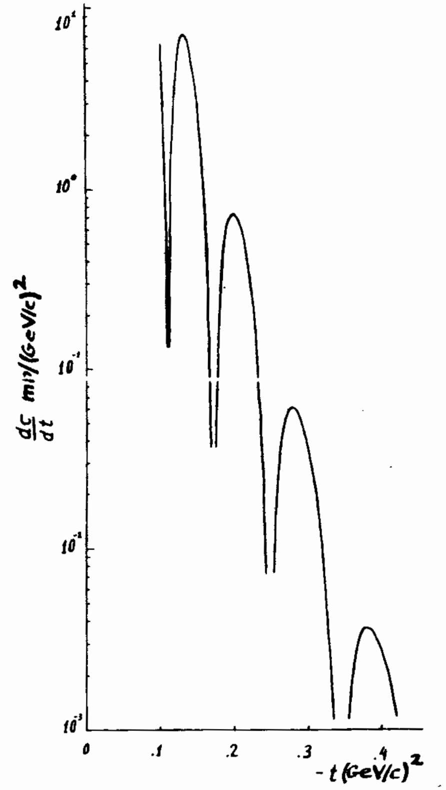

Fig.9. The calculated differential cross section of the $^{40}Ca^{40}Ca$-elastic scattering at high energies.

To answer the question, let's overlook what has been done in the eikonal theory of the inelastic interactions.

Start with the cross-section of all nucleus-nucleus scattering processes accompanied by new particle production which according to basic principles of the eikonal approximation is determined by the following expression

$$\sigma^{p}_{AB} = \int d^2b \{1 - \exp[-\chi(\sigma, T_A, T_B)]\}, \qquad (4)$$

where σ is the inelastic nucleon-nucleon scattering cross section. The production cross section σ^{p}_{AB} can be represented as a sum of the cross sections of processes with different number ν of the inelastic nucleon-nucleon collisions /13/

$$\sigma^{p}_{AB} = \sum_{\nu=1} \sigma_\nu ,$$
$$\sigma_\nu = \frac{(-\sigma)^\nu}{\nu!} \int d^2b \frac{d^\nu}{d\sigma^\nu} e^{-\chi(\vec{b})} . \qquad (5)$$

Notice that each term of the expansion (5), is, in fact, the cross section of the processes with fixed number of the inelastic interactions, but with different numbers of the elastic rescatterings of the constituent nucleons.

It's more difficult to select from each σ_ν the cross sections of different processes. The general solution of this problem was given in paper /14/. From it we have, for example, for $^4He\,^4He$-reactions at ISR energy that one inelastic nucleon-nucleon collision occurs in 47% of all inelastic interactions /15/. Two inelastic nucleon-nucleon collisions occur in 24.7%; three collisions, in 14.1%, and so on. σ_ν, σ_ν and others are subdivided into the cross sections of different processes given in the table and shown in fig.10. Each interaction process like that shown in fig.1 can be represented by a two-coloured graph, or by the edge graph of the two-coloured graph. Some of such edge graphs are presented in fig.10. First of them is in correspondence with the processes with one inelastic collisions. The second one corresponds to the processes with two independent, parallel inelastic interactions. The third one - to the processes in which one of the nucleons of nucleus B collides with two nucleons of nucleus A, and so on.

From the table we can see that in the most cases of the $^4He\,^4He$ interactions there take place the processes analogical to those in the hadron-nucleus collisions. In the processes with a great number of inelastic interactions the processes dominate, having no analogy in the hadron-nucleus collisions (graphs 9,15,16,19-22 of fig.10). Here we can expect new phenomena.

Note that in the collisions of heavy ions multi-scattering processes are realized more often than in the interactions of light nuclei.

Table*

Cross sections of different processes represented in fig.10 (mb)

i	1	2	3	4	5	6	7	8	9	10
$C^{(i)}$	120.9	19.95	21.91	21.91	3.50	3.50	6.86	6.86	13.74	1.96
i	11	12	13	14	15	16	17	18	19	20
$C^{(i)}$	0.283	0.283	0.639	0.639	2.90	2.90	0.307	0.307	3.86	1.32
i	21	22	23	24	25	26	27	28		
$C^{(i)}$	1.92	1.92	0.602	0.602	1.38	0.053	1.17	1.04		

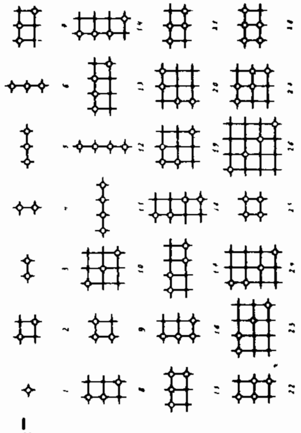

Fig.10. The edge graphs represented different scattering processes in the elastic $^4He\,^4He$-interactions.

*i corresponds to number of graph in fig.10.

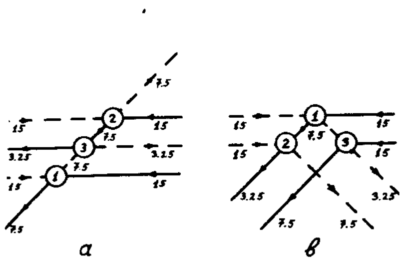

Fig.11. Two processes presented by graph 9 of fig.10. The oriented lines correspond to the nucleons of the "beam" and "target" nuclei. The numbers at lines give values of the longitudinal nucleon momentum in the naive approximation before and after elementary collisions. The numbers in circles indicate the time-order of elementary interactions.

Besides, if in the optical limit on A and B, we have

$$\sigma^{(1)} = \int d^2b\, e^{-\chi(\vec{b})} \frac{1}{\sigma} \int d^2s\, u\, z$$

$$\sigma^{(3)} = \int d^2b\, e^{-\chi(\vec{b})} \frac{1}{\sigma} \int d^2s\, u\, z^2/2$$

$$\sigma^{(4)} = \int d^2b\, e^{-\chi(\vec{b})} \frac{1}{\sigma} \int d^2s\, u^2 z/2$$

$$\sigma^{(2)} = \frac{\sigma^2}{2!} \int d^2b \frac{d^2}{d\sigma^2} e^{-\chi(\vec{b})} - \sigma^{(3)} - \sigma^{(4)}$$

$$\sigma^{(5)} = \int d^2b\, e^{-\chi(\vec{b})} \frac{1}{\sigma} \int d^2s\, u\, z^3/3!$$

$$\sigma^{(9)} = \int d^2b\, e^{-\chi(\vec{b})} \frac{1}{\sigma} \int d^2s\, u^2 z^2,$$

where u and z are solutions of eqs. (3) at $x = \sigma T_A(\vec{s})$, $y = \sigma T_B(\vec{b}-\vec{s})$ and the functions u and z are of the same order of smallness, so the two last expressions differ only by coefficient 1/3!. It means that the processes represented by graph 9 of fig.10 and analogous to them dominate in the heavy-ion collisions. Summarizing all what have been said above, one concludes: in the nucleus-nucleus interactions at high energies, especially in the interactions of heavy ions we can investigate the new type of reactions.

Let's look more carefully on the process presented by graph 9 of fig.10. For this purpose we redraw graph 9 in a new form (fig.11). Now a simple comsideration of the nucleons spectra shows that nucleons very often will fall into the central region. Due to the multiscattering they will have relatively large transversal momenta. Because it's expected that such processes will play an essential role in the nucleus-nucleus

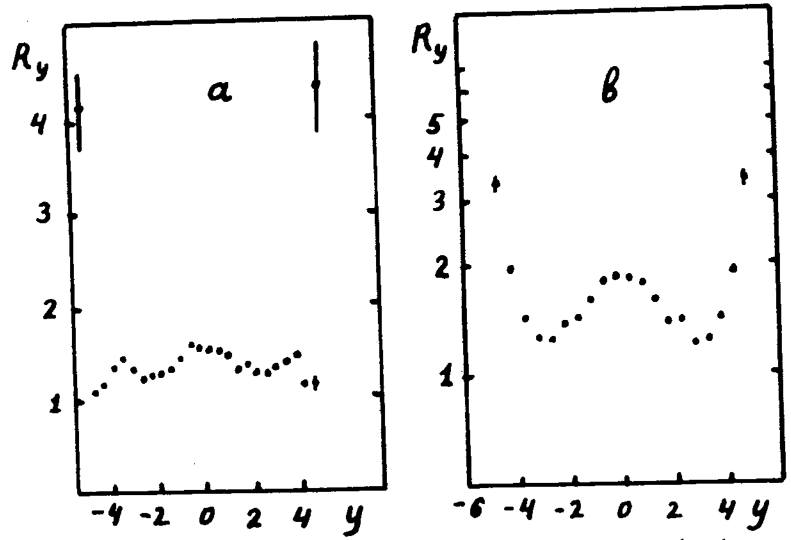

Fig.12. The ratio of particle densities in $^4He^4He$ collisions to pp-interactions versus rapidity y for positive-charged particles. The points are the data of ref./16/ and ref./1/ (figs.a and b, respectively).

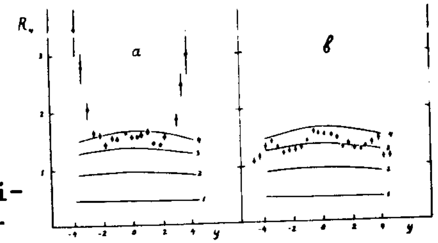

Fig.13. The ratio of negative and positive-charged particle densities (figs.a and b, respectively) in $^4He^4He$-interactions to pp-collisions. The points are the data from paper/16/; the lines, the calculations from ref./15/ of the contributions of one, one-two, one-three, one-four inelastic nucleon-nucleon interactions in scattering processes (curves 1,2,3,4, respectively).

interactions, we arrive at the prediction: in the inelastic collisions of heavy ions many baryons will be produced in the central region with high $P_\perp$.

This can explain the difference between two data sets/1,16/ on $^4He^4He$-interactions at the ISR (fig.12). First of then concerns the characteristics of all secondaries; whereas the other/16/, the particles with $P_\perp > 0.2$ GeV/c. As can be seen from the data[16] on positive-charged particles, the bump in the central region is here bigger than in the data[1]. As in this experiment protons were not distinguished from π^+-mesons and the spectra of π^--mesons have no any bright peculiarity (fig.13), we have to conclude that the indicated irregularity is caused by the protons, in agreement with the prediction.

Will it be true in the heavy-ions collisions the future will show.

SUMMARY

The eikonal theory can describe many features of nucleus-nucleus interactions at high energies. On its base, knowing situations in the hadron-hadron and hadron-nucleus physics, we can predict where new phenomena may appear.

REFERENCES

1. Faessler M.A. CERN, EP/81-61, Geneva, 1981.
2. Uzhinskii V.V. JINR, P2-81-789, Dubna, 1981.
3. Azhgirey L.S. et al. Nucl.Physi, 1978, A305, p.397; Yad.Fiz., 1978, 28, p.124.
4. Alberi G., Goggi G. Phys.Rep., 1981, 74, p.3.
5. Andreev I.V. FIAN preprint No.92, Moscow, 1976; Andreev I.V., Chernov A.V. Yad.Fiz., 1978, 28, p.447.
6. Pak A.S. et al. JETP Lett., 1978, 28, p.314.
7. Franco V., Varma G.K. Phys.Rev., 1978, C18, p.349.
8. Czyz W., Maximon L.C. Ann.of Phys. (N.Y.), 1969, 52, p.59.
9. Chaumeaux A. et al. Nucl.Phys., 1976, A267, p.413.
10. Alkharov G.D. et al. Nucl.Phys., 1977, A280, p.365.
11. Pak A.S. et al. Yad.Fiz., 1979, 30, p.102.
12. Tarasov A.V. Abstracts of Contributed Papers to XVIII Int.Conf. on High Energy Physics and Nuclear Structure. Vancouver, 1979.
13. Uzhinskii V.V. JINR, E2-81-219, Dubna, 1981.
14. Uzhinskii V.V. JINR, E2-81-331, Dubna, 1981.
15. Uzhinskii V.V. JINR, P2-81-780, Dubna, 1981.
16. Bell W. et al. CERN, EP/81-61, Geneva, 1981.

Received by Publishing Department
on June 8 1982.

SUBJECT CATEGORIES OF THE JINR PUBLICATIONS

Index	Subject
1.	High energy experimental physics
2.	High energy theoretical physics
3.	Low energy experimental physics
4.	Low energy theoretical physics
5.	Mathematics
6.	Nuclear spectroscopy and radiochemistry
7.	Heavy ion physics
8.	Cryogenics
9.	Accelerators
10.	Automatization of data processing
11.	Computing mathematics and technique
12.	Chemistry
13.	Experimental techniques and methods
14.	Solid state physics. Liquids
15.	Experimental physics of nuclear reactions at low energies
16.	Health physics. Shieldings
17.	Theory of condenced matter
18.	Applied researches
19.	Biophysics

Ужинский В.В. E2-82-426

Некоторые результаты эйкональной теории ядро-ядерного рассеяния

Суммированы главные результаты эйкональной теории ядро-ядерного рассеяния при высоких энергиях, такие, как описание упругого рассеяния и реакций возбуждения, предсказания эффектов неупругих экранировок в упругом рассеянии и доминирования новых процессов в ион-ионных неупругих взаимодействиях, не имеющих аналога в адрон-ядерных столкновениях.

Работа выполнена в Лаборатории вычислительной техники и автоматизации ОИЯИ.

Препринт Объединенного института ядерных исследований. Дубна 1982

Uzhinskii V.V. E2-82-426

Some Results of the Nucleus-Nucleus Scattering Eikonal Theory

The main results of the eikonal theory are summarized such as: description of the elastic scattering and the excitation reactions in high energy nucleus-nucleus collisions; predictions of inelastic shadowing effects in elastic scattering and of the domination of new processes in ion-ion inelastic interactions having no analogy in hadron-nucleus collisions.

The investigation has been performed at the Laboratory of Computing Techniques and Automation, JINR.

Preprint of the Joint Institute for Nuclear Research. Dubna 1982